Absorption Coefficients of Marine Waters: Expanding Multiband Information to Hyperspectral Data

Zhong Ping Lee, W. Joseph Rhea, Robert Arnone, and Wesley Goode

***Abstract*—For many oceanographic studies and applications, it is desirable to know the spectrum of the attenuation coefficient. For water of the vast ocean, an effective way to get information about this property is through satellite measurements of ocean color. Past and present satellite sensors designed for ocean-color measurements, however, can only provide data in a few spectral bands. A tool is needed to expand these multiband measurements to hyperspectral information. The major contributors to the attenuation coefficient are absorption and backscattering coefficients. The spectral backscattering coefficient can generally be well described with a couple of parameters, but not so for the spectral absorption coefficient. In this paper, based on available hyperspectral absorption data, spectral-transfer coefficients are developed to expand multiband absorption coefficients to hyperspectral (400–700 nm with a 10-nm step) absorption spectrum. The derived transfer coefficients are further applied to data from field measurements to test their performance, and it is found that modeled absorption matches measured absorption very well (∼5% error). These results indicate that when absorption and backscattering coefficients are available at multiple bands, a hyperspectral attenuation-coefficient spectrum can now be well constructed.**

***Index Terms*—Absorption coefficient, hyperspectral, multispectral, remote sensing.**

I. Introduction

FOR STUDIES of heat budget [1], [2] and photosynthesis [3]–[5] in the ocean and many other applications [6]–[8], it is required to know light intensity at depth. Current methods usually use photosynthetic available radiation (PAR) [9] at surface and the diffuse attenuation coefficient of PAR ($K_{\rm PAR}$) for its estimation [10], [11]. This approach cannot provide a measure of light quality (measured by the spectrum of PAR), which is important for analyzing the effectiveness of light usage by phytoplankton [9]. To better describe the light quality and intensity at depth, it is required to know spectral PAR and spectral attenuation coefficient ($K_d(\lambda)$) [3], [12].

Currently, there are two approaches in ocean-color remote sensing to get spectral $K_d(\lambda)$ of the world oceans. Approach 1 [$K_d(\lambda)$] is empirically related to the chlorophyll concentrations ($[C]$) [13], with $[C]$ empirically derived from measurements of ocean color [14]. Approach 2 [$K_d(\lambda)$] is empirically related to the values of $K_d(490)$ (K_d at 490 nm), with $K_d(490)$ empirically derived from measurements of ocean color [15]–[17]. For the two approaches, there are some significant limitations. For Approach 1, Mobley [18] has pointed out that, even for Case-1 waters [19], there is a factor of 2 error in $K_d(450)$ that were the empirically derived using known $[C]$ values [13]. This is simply due to the fact that, in general, water's attenuation coefficients are determined not only by pigment concentrations, but also by other constituents that are dissolved or suspended in waters. Wide deviations are not surprising when variation of K_d is empirically simplified to the variation of $[C]$ [13], [20]. Note that a 30% error in K_d can result in a factor of 2 error in $E_d(z_{10\%})$ where irradiance (E_d) is 10% of its surface value. A factor of 2 error in K_d will certainly lead to significant errors in derived $E_d(z)$ values.

For Approach 2, the single-variant table was developed for $K_d(490)$ less than 0.16 m^{-1} [16]. This range covers most of the oceanic waters, but many coastal waters have $K_d(490)$ greater than this limit [21]. More importantly, the empirically derived $K_d(490)$ itself contains large uncertainties, especially for coastal waters [22].

To overcome the limitations of these empirical approaches and to improve the accuracy of estimating values of K_d, it is necessary to apply analytical approaches to the remotely measured data. For such an objective, Lee *et al.* [23] have recently developed a quasi-analytical algorithm to derive water's absorption and backscattering coefficients from remote sensing reflectance. Incorporating these values into the K_d model of Gordon [24], K_d can be calculated semianalytically from measurements of ocean color.

Past and current satellite sensors, however, have only a few spectral bands designed for ocean-color measurements. Such a configuration limits the spectral K_d that can be semianalytically derived. This limited spectral K_d is insufficient for characterizing the light spectra at depth, and insufficient for determining the optimal spectral window for light penetration [25], [26]. To know detailed spectral information of K_d or to get K_d at wavelengths that do not exist in the current suite of bands, a tool is needed for accurate spectral interpolation or extrapolation from K_d of existing bands. It is noticed that the major contributors to K_d are absorption and backscattering coefficients [24], [27]. Since spectrum of backscattering coefficient can be well described with a couple of parameters [28], [29], what needed is a system or tool to transfer absorption values derived at the satellite bands to a spectrum of absorption coefficient. For this purpose, in an approach similar to Austin and Petzold's [16], spectral transfer coefficients (STCs) are developed to expand

Manuscript received April 12, 2004; revised September 16, 2004. This work was supported in part by the Naval Research Laboratory's Basic Research P.E. 06010115N "Hyperspectral Characterization of the Coastal Zone" and in part by the National Aeronautics and Space Administration's Biological Oceanography Program "Evaluation of the EO-1 (Hyperion and ALI) for applications in the Coastal Ocean."

Z. P. Lee, R. Arnone, and W. Goode are with the Naval Research Laboratory, Stennis Space Center, MS 39529 USA (e-mail: zplee@nrlssc.navy.mil).

W. J. Rhea is with the Naval Research Laboratory, Washington, DC 20375 USA.

Digital Object Identifier 10.1109/TGRS.2004.839815

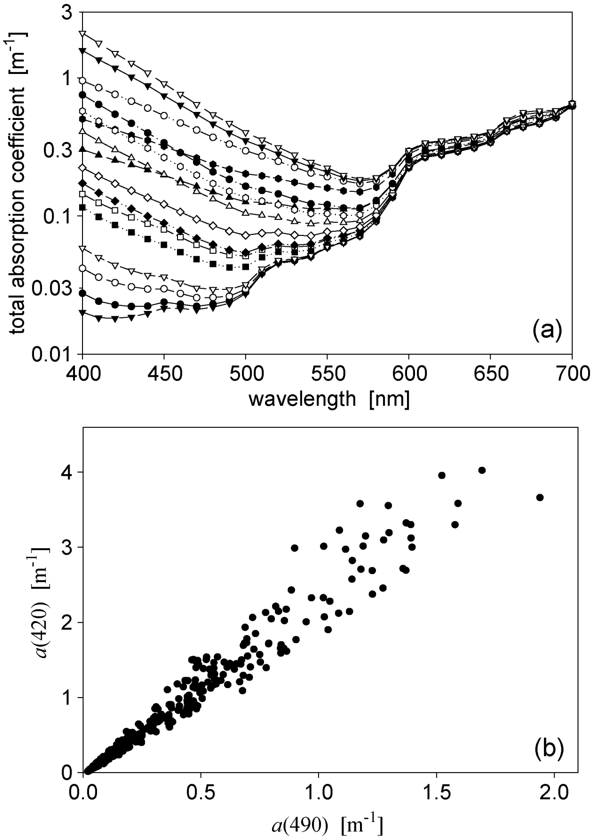

Fig. 1. (a) Examples of absorption spectrum of the dataset (from IOCCG). (b) Ranges and variations of $a(420)$ and $a(490)$ of the dataset.

TABLE I
SPECTRAL TRANSFER COEFFICIENTS FOR CZCS BANDS

wavelength	β(440)	β(520)	β(550)
400	2.1961	-5.5881	4.8369
410	1.7743	-3.4273	2.9711
420	1.4872	-2.2136	2.019
430	1.1904	-0.2205	-0.19
440	1	0	0
450	0.7708	0.5962	-0.4123
460	0.6213	0.5553	-0.1189
470	0.4082	1.3204	-0.7344
480	0.2529	1.8066	-1.1856
490	0.1951	1.6192	-0.9602
500	0.1314	1.32	-0.5303
510	0.0709	1.022	-0.1046
520	0	1	0
530	-0.0031	0.582	0.4451
540	-0.0006	0.2074	0.8402
550	0	0	1
560	-0.0026	-0.1519	1.0912
570	0.0088	-0.2727	1.1247
580	-0.0323	-0.0192	0.8368
590	-0.035	-0.0787	0.8807
600	-0.0218	-0.1544	0.8786
610	-0.051	-0.0098	0.7515
620	-0.0359	-0.2081	0.9741
630	-0.0377	-0.1755	0.8985
640	-0.045	-0.2215	0.9819
650	-0.045	-0.1732	0.8743
660	-0.0273	-0.3531	1.141
670	-0.0029	-0.1738	0.9039
680	-0.0029	-0.1754	0.8432
690	-0.019	-0.2996	0.8741
700	-0.0068	-0.3613	0.7664

multiband absorption coefficients to hyperspectral absorption spectrum.

After the development of the transfer coefficients, the approach and the STC are applied to absorption data obtained from field measurements to test its performance. This testing dataset has no relation to the development of the STC, and promising results are obtained.

II. DATA AND APPROACH

In order to expand multiband values to hyperspectral data, absorption coefficient is expressed as

$$a(\lambda_j) = a_w(\lambda_j) + \sum_{i=1}^{n} \beta_{ij} \left(a(\lambda_i) - a_w(\lambda_i)\right) \qquad (1)$$

where λ_j is the wavelength at the jth band. Values of β_{ij} are the spectral transfer coefficients (STC) that need to be derived, and $a(\lambda_i)$ is the absorption coefficient at the ith band and assumed known from measurements. a_w is the absorption coefficient of pure water and is taken from Pope and Fry [30].

With an aim to apply the results to data collected by the Coastal Zone Color Scanner (CZCS) or the Moderate Resolution Imaging Spectrometer (MODIS), two sets of STC are developed to expand CZCS or MODIS absorption coefficients to hyperspectral spectrum. For CZCS, n is 3 as only 440, 520, and 550 nm exist for ocean studies; therefore, λ_i are 440, 520, and 550 nm, respectively. For MODIS, n is 5 and λ_i are 410, 440, 490, 530, and 550, respectively. Wavelengths longer than 550 nm exist for both CZCS and MODIS sensors. Those bands are excluded in the STC derivation, simply because the absorption coefficients at those bands are in general dominated by the contribution of pure water and quite insensitive to the variation of constituents in the water. Note that an algorithm has already been developed to analytically derive $a(\lambda_i)$ from remote sensing reflectance [23]. So, in this study, the focus is on expanding multiband $a(\lambda_i)$ data to hyperspectral $a(\lambda_j)$ spectrum.

To derive the values of hyperspectral β_{ij}, a large dataset that covering wide range of absorption spectra is required. Due to instrument and measurement limitations, however, such a dataset constructed from field does not yet exist. To overcome this limitation, we utilized the absorption dataset [31] adopted by the International Ocean Color Coordinating Group (IOCCG). The dataset has 500 synthesized $a(\lambda_j)$ spectra covering a wavelength range of 400–700 nm with a step of 10 nm, and the absorption at 440 nm has a range of 0.016–3.17 m^{-1}.

This dataset was synthesized and provided by a working group under the IOCCG. The synthesis of the $a(\lambda_j)$ spectra [31] was based on ocean-optics theory [18], [32]–[34] and extensive field measurements [35]–[38]. Briefly, absorption coefficients were determined by

$$a(\lambda_j) = a_w(\lambda_j) + a_{\mathrm{ph}}(\lambda_j) + a_{\mathrm{g}}(\lambda_j) + a_{\mathrm{dm}}(\lambda_j) \qquad (2)$$

with values of $a_w(\lambda_j)$ taken from Pope and Fry [30], and values of $a_{\mathrm{ph,g,dm}}(\lambda_j)$ synthesized by a set of wide-range

TABLE II
SPECTRAL TRANSFER COEFFICIENTS FOR MODIS BANDS

wavelength	β(410)	β(440)	β(490)	β(530)	β(550)
400	1.6451	-0.9809	0.4638	1.235	-1.6084
410	1	0	0	0	0
420	0.5366	0.564	-0.176	0.0589	0.0461
430	0.3438	0.5289	0.2006	0.0367	0.0003
440	0	1	0	0	0
450	0.0431	0.5941	0.5499	-0.1254	-0.1379
460	-0.0176	0.4643	0.665	0.1723	-0.3278
470	-0.0145	0.2845	0.8362	-0.0341	-0.0655
480	0.0012	0.0846	1.0269	-0.1105	-0.0052
490	0	0	1	0	0
500	0.0218	-0.0861	0.8282	0.3051	-0.0439
510	-0.0083	-0.0109	0.414	0.6789	-0.0007
520	0.0203	-0.0651	0.2212	0.9254	-0.0562
530	0	0	0	1	0
540	-0.0092	0.0299	-0.0596	0.5319	0.5119
550	0	0	0	0	1
560	0.0304	-0.0676	0.0438	-0.3632	1.3508
570	0.0051	-0.0097	-0.0143	-0.1324	0.9737
580	-0.0187	0.0326	-0.1143	0.0849	0.7885
590	-0.0366	0.0696	-0.1511	0.206	0.6006
600	-0.0326	0.0624	-0.1628	0.1901	0.5946
610	-0.0926	0.2187	-0.3501	0.4137	0.3814
620	-0.2064	0.5258	-0.781	0.6058	0.466
630	-0.1904	0.4832	-0.6237	0.4509	0.3611
640	-0.2057	0.548	-0.749	0.5009	0.3621
650	-0.2434	0.6824	-0.9677	0.4769	0.5066
660	-0.039	0.1072	-0.4332	0.5823	0.484
670	-0.6708	1.759	-2.06	0.8171	0.7173
680	-0.5688	1.4889	-1.8248	1.4044	-0.1358
690	-0.1554	0.4799	-0.9513	0.5347	0.6663
700	-0.0213	0.102	-0.3731	0.2195	0.4362

optical properties [31]. Here, subscripts ph, g, and dm are for phytoplankton, gelbstoff [or colored dissolved organic matter (CDOM)], and detritus/minerals, respectively. In the synthesis of the $a(\lambda_j)$ dataset, $a_{\mathrm{ph}}(440)$ varied from 0.0056–0.42 m^{-1}, while the spectral shapes of $a_{\mathrm{ph}}(\lambda_j)$ were randomly chosen from field measurements. Further, the magnitude and spectral shape for both $a_{\mathrm{g}}(\lambda_j)$ and $a_{\mathrm{dm}}(\lambda_j)$ were varied randomly in accordance with field measurements. Therefore, the synthesized $a(\lambda_j)$ dataset covers a wide range of magnitudes and spectral curvatures, representing a majority of possible absorption spectra that could be encountered in the field. As examples, Fig. 1(a) presents a few selected absorption spectra from the dataset, with Fig. 1(b) showing the values of $a(420)$ versus $a(490)$ for the 500 points.

With this dataset, values of β_{ij} were derived by minimizing the difference between known $a(\lambda_j)$ and (1)-derived $a(\lambda_j)$. Tables I and II present the β_{ij} values for configurations of CZCS and MODIS sensors. Similarly, values of β_{ij} could be derived for other sensors, such as the SeaWiFS.

III. RESULTS OF THE MULTIVARIANT EXPANSION

As examples to show the performance of $a(\lambda_j)$ derived from multivariant expansion, Fig. 2 presents (1)-derived $a(420)$ versus known $a(420)$, while Fig. 3 presents examples of multivariant expanded $a(\lambda_j)$ versus true $a(\lambda_j)$. The modeled $a(420)$ in Fig. 2 was derived using $a(440, 520, 550)$, i.e., based on the CZCS bands. Clearly, these results indicate that hyperspectral total absorption could be well and effectively derived if values of $a(\lambda_i)$ are available. Especially, for a sensor with a band around 410 nm, the expanded $a(\lambda_j)$ matches the true $a(\lambda_j)$ excellently [Fig. 3(b)] for the 400–700-nm range. With this $a(\lambda_j)$ spectrum and spectrum of backscattering coefficient from remote sensing [23], a hyperspectral K_d can then be semianalytically derived [24], and accurate E_d spectrum at depth can be calculated.

To demonstrate increased accuracy in estimated $a(\lambda_j)$ with extra inputs, Fig. 4 presents the average and maximum errors for each wavelength, with Fig. 4(a) for averaged error and Fig. 4(b) for maximum error. Error for each $a(\lambda_j)$ is simply calculated as

$$\mathrm{error} = \frac{|a(\lambda_j)_{\mathrm{model}} - a(\lambda_j)_{\mathrm{known}}|}{a(\lambda_j)_{\mathrm{known}}} \times 100\% \qquad (3)$$

and the average error is a simple arithmetic mean for each λ_j.

Clearly, if $a(\lambda_j)$ is simply expanded using $a(490)$ as that of Austin and Petzold [16], errors can reach as high as 50% at 400 nm, though errors are smaller for wavelengths around 490 nm. This is due to that $a(490)$ alone cannot well represent the contributions of phytoplankton and CDOM in the shorter wavelengths. Change the derivation from single input to multiple inputs, significant improvements were achieved in deriving $a(\lambda_j)$, as both average and maximum errors are reduced. Especially, with the MODIS configuration, the errors are greatly reduced for wavelengths from 400–650 nm.

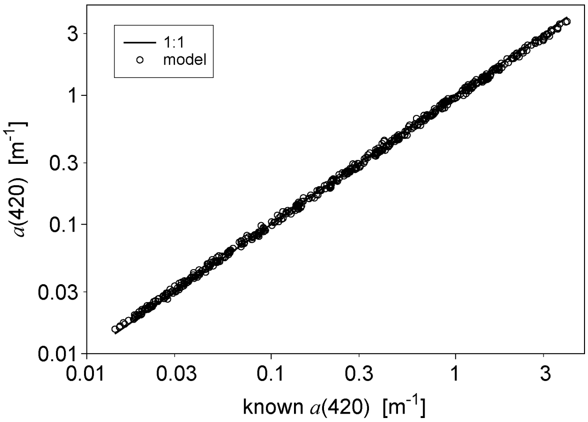

Fig. 2. Values of $a(420)$ modeled using $a(440, 520, 550)$ compared with known values of $a(420)$. 440&520&550 is the spectral configuration of the CZCS.

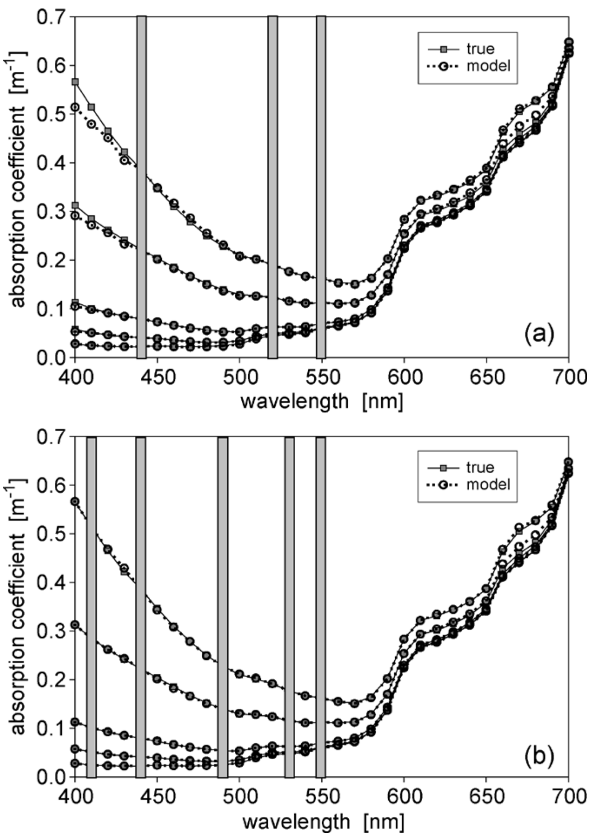

Fig. 3. (a) Examples of $a(\lambda j)$ modeled using $a(440, 520, 550)$ compared with known values of $a(\lambda j)$. Vertical bars indicate the location of the CZCS bands. (b) Examples of $a(\lambda j)$ modeled using $a(410, 440, 490, 530, 550)$ compared with known values of $a(\lambda j)$. Vertical bars indicate the location of the MODIS bands.

The slightly larger errors (∼3% average error and ∼15% maximum error) around 670 nm are due to the fact that, in this multivariant expansion, the longest wavelength used for $a(\lambda_i)$ is 550 nm, which is imperfect to refer the chlorophyll contribution at 670 nm (the red peak). Though $a(440)$ contains information of chlorophyll contribution, $a(440)$ also contains independent contributions from CDOM and detritus, and the chlorophyll contributions at 440 and 670 nm do not follow a fixed relationship. This imperfection is not serious for oceanic and most coastal waters as larger error (∼15%) happens only to very high absorbing waters $(a(440) \sim 2.2\ \mathrm{m}^{-1})$ where the contribution from chlorophyll is quite pronounced at 670 nm (∼40% of the total absorption coefficient is from chlorophyll). For oceanic and most coastal waters, this contribution is small at 670 nm.

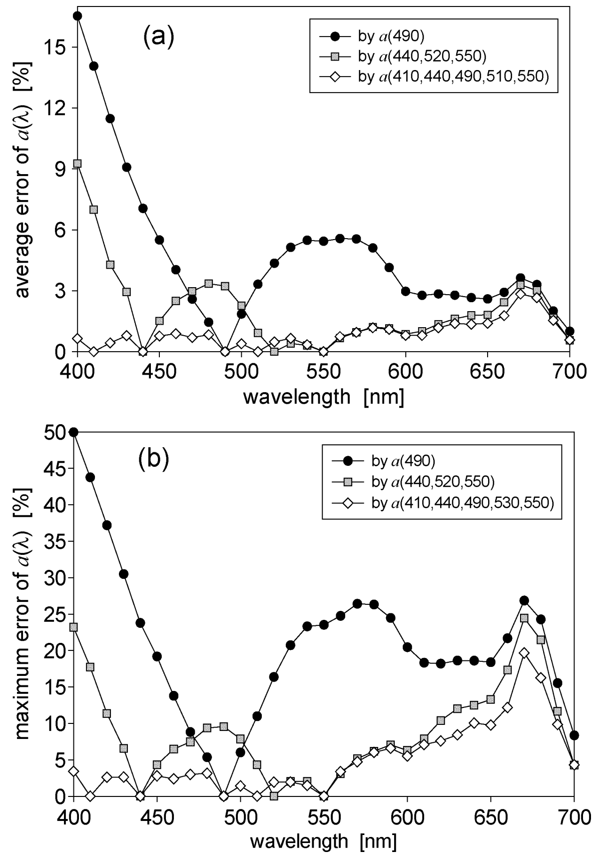

Fig. 4. (a) Average error between modeled $a(\lambda j)$ and known $a(\lambda j)$ for three different configurations of inputs. (b) Maximum model error between modeled $a(\lambda j)$ and known $a(\lambda j)$ for three different configurations of inputs.

IV. TEST WITH *IN SITU* DATA

To ensure its applicability of the approach and the STC to the real world, it is certainly desirable to know how it performs with data from field measurements. For this purpose, we applied the three-band expansion (CZCS configuration) to a dataset collected in the field. The data came from two field cruises: Gulf of Mexico in June of 1993 and California coast in April of 2003. Both cruises covered oceanic and coastal waters. For the Gulf of Mexico, absorption coefficients were derived from downwelling diffuse coefficients as presented by Lee *et al.* [39]. In this dataset (total number of data points $(N) = 23$), there were no measurements at 410 nm. For the 2003-California dataset $(N = 57)$, the absorption coefficients were obtained with the AC-9 instrument (WetLabs, Inc.). For this measurement, the instrument was regularly calibrated before, during, and after the cruise, with all procedures performed following the protocols suggested by WetLabs, Inc.

Fig. 5 compares the measured results versus those modeled using $a(440, 520, 555)$, with Fig. 5(a) for $a(410)$ and Fig. 5(b) for $a(490)$. $a(555)$ replaced $a(550)$ as input simply because band location, and no change made to the STC values. Also,

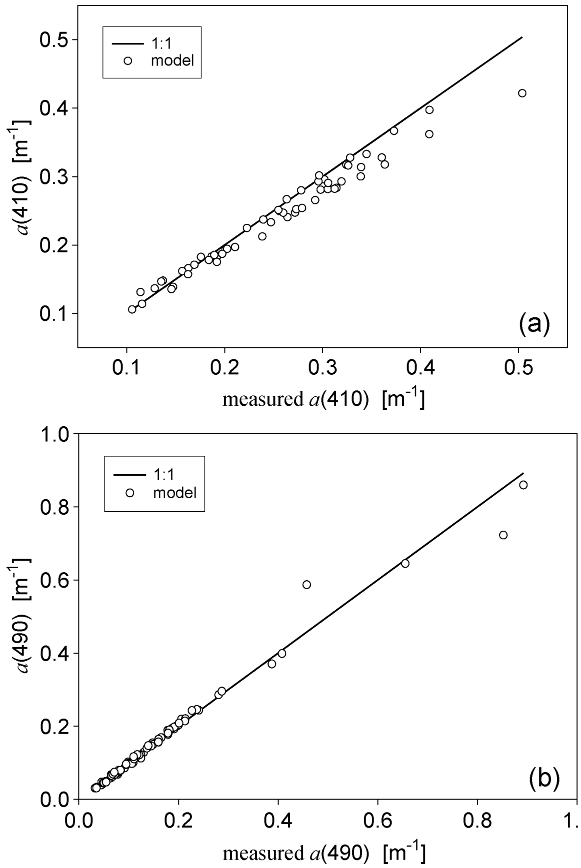

Fig. 5. (a) Values of $a(410)$ modeled using $a(440, 520, 555)$ compared with measured values of $a(410)$. (b) Values of $a(490)$ modeled using $a(440, 520, 555)$ compared with measured values of $a(490)$.

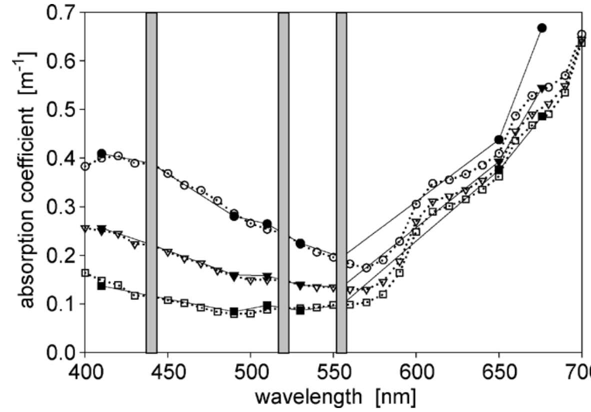

Fig. 6. Examples of constructed hyperspectral $a(\lambda j)$ (open symbol, dotted line) using measured values at three wavelengths (the vertical bar, CZCS configuration). The hyperspectral $a(\lambda j)$ is compared with multiband data (solid symbol, solid line) from AC-9 (Wetlabs, Inc.) measurements.

as there were no measurements at 520 nm, $a(520)$ was taken as an average of $a(510)$ and $a(530)$ that were measured by AC-9. For $a(410)$ ranging from 0.1–0.5 m^{-1} ($N = 57$), the average error is 5.3% (maximum error is 15.4%). For the absorption coefficient at 490 nm (a band that does not exist on CZCS), the average error is 4.5% ($N = 80$, maximum error is 28.4%) for a range of 0.03–0.9 m^{-1}. Note that most of the data points ($N = 75$) are with $a(490) < 0.4$ m^{-1}, where the average error is 4.1%. The average error is 10.2% for the five points with $a(490) > 0.4$ m^{-1}. To visualize the spectral details of hyperspectral $a(\lambda_j)$, Fig. 6 presents a few examples of $a(\lambda_j)$ constructed using $a(440, 520, 555)$, along with multiband $a(\lambda_i)$. Clearly, for the AC-9 bands, values of $a(\lambda_j)$ match those from measurements very well. However, it is the hyperspectral $a(\lambda_j)$ that provides a detailed description of the absorption spectrum, not the multiband data.

These results indicate that the multivariant expansion works well in deriving absorption coefficients at other wavelengths. Also, the close agreements between measured and modeled $a(\lambda_j)$ support the conclusion [40] that for most applications of ocean-color remote sensing, it is not a first-order priority to have a satellite sensor with hyperspectral bands. For high quality observations of the environments, it is more important to have sensors with high signal-to-noise ratio and high spatial resolution.

With the spectral transfer tool and the semianalytical algorithm for remote sensing [23], it is now straightforward to construct hyperspectral K_d spectrum from data derived at the CZCS and/or SeaWiFS/MODIS bands. Such hyperspectral data can be used to analyze its decadal trend and can be used in numerical models to better study the heat budget as well as primary production [41]. It is recognized, however, $a(\lambda_i)$ from satellite sensors will contain errors associated with any satellite system. So $a(\lambda_j)$ derived from satellite data will not be as good as that shown above. To improve this accuracy, it requires well-calibrated sensors, advanced algorithms for atmosphere correction, and robust algorithms for $a(\lambda_i)$ derivation, objectives the community is striving for.

V. Summary

In order to get hyperspectral absorption spectrum from multiband absorption coefficients that are available from CZCS or MODIS measurements, spectral transfer coefficients were empirically derived from a hyperspectral dataset adopted by the IOCCG. The STC were further tested with data from field measurements. For wide dynamic range of absorption coefficients, it is found that the derived absorption coefficients match the measured values very well (~5% average error). These results suggest that hyperspectral absorption can be well constructed from multiband values. As the diffuse attenuation coefficient for downwelling irradiance is made of absorption and backscattering coefficients [24], [27], and spectrum of backscattering coefficient can be well retrieved from remote sensing [23], [42], the spectrum of attenuation coefficient can now be quickly constructed from multiband satellite data. Such information will help the estimation of light quality and intensity at a depth in the ocean, and improve the estimation of heat budget and primary production. Due to the empirical nature of the approach, however, testing the STC with extensive field data is necessary and further improvement is envisioned.

Acknowledgment

The authors thank the Ocean Color Algorithm Group under the IOCCG for the creation of the dataset, and are grateful to the comments of two anonymous reviewers.

REFERENCES

[1] M. R. Lewis *et al.*, "Influence of penetrating solar radiation on the heat budget of the equatorial Pacific Ocean," *Nature*, vol. 347, pp. 543–545, 1990.
[2] A. Morel and D. Antoine, "Heating rate within the upper ocean in relation to its bio-optical state," *J. Phys. Oceanogr.*, vol. 24, pp. 1652–1665, 1994.
[3] S. Sathyendranath *et al.*, "Remote sensing of oceanic primary production: Computations using a spectral model," *Deep-Sea Res.*, vol. 36, pp. 431–453, 1989.
[4] T. Platt *et al.*, "Ocean primary production and available light: Further algorithms for remote sensing," *Deep-Sea Res.*, vol. 35, pp. 855–879, 1988.
[5] J. Marra, C. Langdon, and C. A. Knudson, "Primary production and water column changes and the demise of a Phaeocystis bloom at the marine light-mixed layers site (59° N/21° W, North Atlantic Ocean)," *J. Geophy. Res.*, vol. 100, no. C4, pp. 6633–6644, 1994.
[6] J. T. O. Kirk, *Light and Photosynthesis in Aquatic Ecosystems*. Cambridge, U.K.: Cambridge Univ. Press, 1986.
[7] C. R. McClain *et al.*, "Observations and simulations of physical and biological process at ocean weather station P, 1951–1980," *J. Geophy. Res.*, vol. 101, pp. 3697–3713, 1996.
[8] E. K. Schneider and Z. Zhu, "Sensitivity of the simulated annual cycle of sea surface temperature in the Equatorial Pacific to sunlight penetration," *J. Clim.*, vol. 11, pp. 1932–1950, 1998.
[9] A. Morel, "Available, usable, and stored radiant energy in relation to marine photosynthesis," *Deep-Sea Res.*, vol. 25, pp. 673–688, 1978.
[10] J. C. Ohlmann, D. Siegel, and C. Gautier, "Ocean mixed layer radiant heating and solar penetration: A global analysis," *J. Clim.*, vol. 9, pp. 2265–2280, 1996.
[11] P. A. Rochford *et al.*, "Importance of solar subsurface heating in ocean general circulation models," *J. Geophy. Res.*, vol. 106, pp. 30 923–30 938, 2001.
[12] T. Platt and S. Sathyendranath, "Oceanic primary production: Estimation by remote sensing at local and regional scales," *Science*, vol. 241, pp. 1613–1620, 1988.
[13] A. Morel, "Optical modeling of the upper ocean in relation to its biogenous matter content (Case I waters)," *J. Geophy. Res.*, vol. 93, pp. 10 749–10 768, 1988.
[14] J. O'Reilly *et al.*, "Ocean color chlorophyll algorithms for SeaWiFS," *J. Geophy. Res.*, vol. 103, pp. 24 937–24 953, 1998.
[15] R. W. Austin and T. J. Petzold, "The determination of the diffuse attenuation coefficient of sea water using the coastal zone color scanner," in *Oceanography From Space*, J. F. R. Gower, Ed. New York: Plenum, 1981, pp. 239–256.
[16] ——, "Spectral dependence of the diffuse attenuation coefficient of light in ocean waters," *Opt. Eng.*, vol. 25, pp. 473–479, 1986.
[17] J. L. Mueller and C. C. Trees, "Revised SeaWIFS prelaunch aAlgorithm for diffuse attenuation coefficient K(490). Case studies for SeaWiFS calibration and validation," NASA Goddard Space Flight Center, Greenbelt, MD, NASA Tech Memo. 104566, vol. 41, S. B. Hooker and E. R. Firestone, Eds., 1997.
[18] C. D. Mobley, *Light and Water: Radiative Transfer in Natural Waters*. New York: Academic, 1994.
[19] A. Morel and L. Prieur, "Analysis of variations in ocean color," *Limnol. Oceanogr.*, vol. 22, pp. 709–722, 1977.
[20] A. Morel and S. Maritorena, "Bio-optical properties of oceanic waters: A reappraisal," *J. Geophy. Res.*, vol. 106, pp. 7163–7180, 2001.
[21] J. L. Mueller, "SeaWiFS algorithm for the diffuse attenuation coefficient, K(490), using water-leaving radiances at 490 and 555 nm," in *SeaWiFS Postlaunch Calibration and Validation Analyses*, S. B. Hooker, Ed. Greenbelt, MD: NASA Goddard Space Flight Center, 2000, pt. 3, pp. 24–27.
[22] M. Darecki and D. Stramski, "An evaluation of MODIS and SeaWiFS bio-optical algorithms in the Baltic Sea," *Remote Sens. Environ.*, vol. 89, pp. 326–350, 2004.
[23] Z. P. Lee, K. L. Carder, and R. Arnone, "Deriving inherent optical properties from water color: A multi-band quasianalytical algorithm for optically deep waters," *Appl. Opt.*, vol. 41, pp. 5755–5772, 2002.
[24] H. R. Gordon, "Can the Lambert-Beer law be applied to the diffuse attenuation coefficient of ocean water?," *Limnol. Oceanogr.*, vol. 34, pp. 1389–1409, 1989.
[25] F. E. Hoge, R. N. Swift, and E. B. Frederick, "Water depth measurement using an airborne pulsed neon laser system," *Appl. Opt.*, vol. 19, pp. 871–883, 1980.
[26] H. C. Wong and A. Antoniou, "Two-dimensional signal processing techniques for airborne laser bathymetry," *IEEE Trans. Geosci. Remote Sens.*, vol. 34, no. 1, pp. 57–66, Jan. 1996.
[27] Z. P. Lee, K. P. Du, and R. Arnone, "A model for the diffuse attenuation coefficient of downwelling irradiance," *J. Geophy. Res.*, 2005, to be published.
[28] R. C. Smith and K. S. Baker, "Optical properties of the clearest natural waters," *Appl. Opt.*, vol. 20, pp. 177–184, 1981.
[29] S. Sathyendranath, L. Prieur, and A. Morel, "A three-component model of ocean color and its application to remote sensing of phytoplankton pigments in coastal waters," *Int. J. Remote Sens.*, vol. 10, pp. 1373–1394, 1989.
[30] R. Pope and E. Fry, "Absorption spectrum (380–700 nm) of pure waters: II. Integrating cavity measurements," *Appl. Opt.*, vol. 36, pp. 8710–8723, 1997.
[31] IOCCG-OCAG. (2003) Model, parameters, and approaches used to generate wide range of absorption and backscattering spectra. Int. Ocean Color Coordinating Group. [Online]. Available: http://www.ioccg.org/groups/OCAG_data.html.
[32] H. R. Gordon and A. Morel, *Remote Assessment of Ocean Color for Interpretation of Satellite Visible Imagery: A Review*. New York: Springer-Verlag, 1983, vol. 44.
[33] H. R. Gordon, R. C. Smith, and J. R. V. Zaneveld, "Introduction to ocean optics," *Proc. SPIE*, vol. 208, pp. 1–39, 1980.
[34] J. T. O. Kirk, *Light and Photosynthesis in Aquatic Ecosystems*. Cambridge, U.K.: Cambridge Univ. Press, 1994.
[35] A. Bricaud, A. Morel, and L. Prieur, "Absorption by dissolved organic matter of the sea (yellow substance) in the UV and visible domains," *Limnol. Oceanogr.*, vol. 26, pp. 43–53, 1981.
[36] K. L. Carder *et al.*, "Marine humic and fulvic acids: their effects on remote sensing of ocean chlorophyll," *Limnol. Oceanogr.*, vol. 34, pp. 68–81, 1989.
[37] ——, "Reflectance model for quantifying chlorophyll a in the presence of productivity degradation products," *J. Geophys. Res.*, vol. 96, pp. 20 599–20611, 1991.
[38] C. S. Roesler, M. J. Perry, and K. L. Carder, "Modeling in situ phytoplankton absorption from total absorption spectra in productive inland marine waters," *Limnol. Oceanogr.*, vol. 34, pp. 1510–1523, 1989.
[39] Z. P. Lee *et al.*, "An empirical algorithm for light absorption by ocean water based on color," *J. Geophy. Res.*, vol. 103, pp. 27 967–27 978, 1998.
[40] Z. P. Lee and K. L. Carder, "Effect of spectral band numbers on the retrieval of water column and bottom properties from ocean color data," *Appl. Opt.*, vol. 41, pp. 2191–2201, 2002.
[41] S. Sathyendranath and T. Platt, "The spectral irradiance field at the surface and in the interior of the ocean: A model for applications in oceanography and remote sensing," *J. Geophy. Res.*, vol. 93, pp. 9270–9280, 1988.
[42] H. Loisel and D. Stramski, "Estimation of the inherent optical properties of natural waters from the irradiance attenuation coefficient and reflectance in the presence of Raman scattering," *Appl. Opt.*, vol. 39, pp. 3001–3011, 2000.

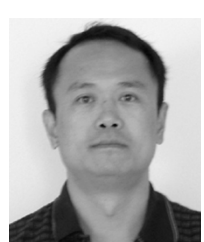

Zhong Ping Lee received the B.S. degree in optical physics from Sichuan University, Chengdu, China, in 1984, the M.S. degree in laser application from the Ocean University of China, Qingdao, China, in 1987, and the Ph.D. degree in ocean-color remote sensing from the University of South Florida, St. Petersburg, in 1994.

He is currently with the Oceanography Division of the Naval Research Laboratory, Stennis Space Center, MS. He was a Research Associate with Dr. Kendall L. Carder at the College of Marine Science, University of South Florida. He has conducted research in ocean-color remote sensing for both optically deep and shallow waters and has developed models and algorithms for retrieving important environmental properties from the observation of water color.

W. Joseph Rhea received the B.S. degree in oceanography from the University of Washington, Seattle, WA, in 1986.

He is currently with the Remote Sensing Division, Naval Research Laboratory, Washington, DC, with research studies focusing on the inherent optical properties of coastal water. He worked for the Oceanographic and Meteorological Science Group of Envirosphere Company from 1985 to 1988, where his primary research involved the study of physical oceanographic processes and yearly sea ice freeze/thaw cycles along the north slope of Alaska. From 1988 to 1994, he was with the NASA Jet Propulsion Laboratory, Pasadena, CA, where he was responsible for a collection of underwater optical data using one of the first bio-optical profiler systems. While there, he was a participant in all early Joint Global Ocean Flux Study cruises, as well as over a dozen experiments scattered around the U.S.

Robert Arnone received the B.S. degree in geology from Kent State University, Kent, OH, the M.S. degree in geophysical sciences from the Georgia Institute of Technology, Atlanta, and advanced studies in coastal oceanography from Louisiana State University, Baton Rouge.

He is currently the Head of the Ocean Science Branch, Oceanography Division, Naval Research Laboratory (NRL), Stennis Space Center, MS. He is leading over 50 oceanographers focusing on: 1) ocean optical processes and remote sensing; 2) biological modeling of coupled dynamical processes; and 3) fine-scale and meso-scale physical processes. He serves on ocean science teams for NASA, NOAA, and U.S. Navy programs and U.S. delegations in coastal oceanography. He is also an Adjunct Faculty Member with the University of Southern Mississippi, Hattiesburg, and the University of Southern Alabama, Mobile.

Mr. Arnone is a Board Member of the Alliance for Marine Remote Sensing. He has received awards for naval honors for science transitions and NRL Alan Berman publication awards. He has received Navy patents and NASA honors for astronaut training programs.

Wesley Goode received the B.S. degree in electronic engineering from the University of Southern Mississippi, Hattiesburg, in 1993.

He is currently an Engineering Technician with the Ocean Optics Section, Naval Research Laboratory (NRL), Stennis Space Center, MS. He has over ten years of experience in optical instrumentation, satellite remote sensing, and data and imagery processing and analysis. He is currently the Lead Person responsible for collection and processing of NRL's optical *in situ* data and is also responsible for the operation of NRL's real-time satellite receiving system which collects local AVHRR and SeaWiFS data.